*Nano Research* 2016, 9(7): 2182–2189
DOI 10.1007/s12274-016-1107-9
**Research Article**
ISSN 1998-0124
CN 11-5974/O4

# Growth of large-area aligned pentagonal graphene domains on high-index copper surfaces

Kailun Xia[1,2], Vasilii I. Artyukhov[3], Lifei Sun[1], Jingying Zheng[1], Liying Jiao[1], Boris I. Yakobson[3], and Yingying Zhang[1,2] (✉)

[1] *Department of Chemistry, Tsinghua University, Beijing 100084, China*
[2] *Center for Nano and Micro Mechanics, Tsinghua University, Beijing 100084, China*
[3] *Department of Materials Science and Nano Engineering, Rice University, Houston, TX 77005, USA*

**Received:** 17 February 2016
**Revised:** 11 April 2016
**Accepted:** 14 April 2016



**KEYWORDS**
pentagonal graphene,
copper foil,
high index plane,
chemical vapor deposition,
large area

## ABSTRACT

Single-crystal graphene domains grown by chemical vapor deposition (CVD) intrinsically tend to have a six-fold symmetry; however, several factors can influence the growth kinetics, which can in turn lead to the formation of graphene with different shapes. Here we report the growth of oriented large-area pentagonal single-crystal graphene domains on Cu foils by CVD. We found that high-index Cu planes contributed selectively to the formation of pentagonal graphene. Our results indicated that lattice steps present on the crystalline surface of the underlying Cu promoted graphene growth in the direction perpendicular to the steps and finally led to the disappearance of one of the edges forming a pentagon. In addition, hydrogen promoted the formation of pentagonal domains. This work provides new insights into the mechanism of graphene growth.

## 1 Introduction

Graphene has attracted much attention due to its unique structure, superior properties [1], and potential applications [2–7]. Metal-assisted chemical vapor deposition (CVD), especially using copper (Cu) foils as substrates, has been widely investigated for the growth of high quality graphene [8–10]. Single-crystal graphene grown on Cu shows various shapes such as, hexagonal [11, 12], snowflake [13], rectangular [14] and triangular [15]. Theoretical and experimental studies revealed that both the CVD process conditions and the substrate crystallography influence the shape of the obtained graphene [14–17]. The crystallographic plane of Cu that is best matched with graphene, is the (111) plane [14, 18], which has an interatomic spacing of 0.148 nm, close to the graphene C–C distance of 0.142 nm (4% mismatch). For other Cu planes, the mismatch between graphene and the Cu lattice is higher; the lower atomic density and the presence of a large number of steps on the surface lead to the distortion of the graphene domains by altering the

Address correspondence to yingyingzhang@tsinghua.edu.cn

growth rate [17]. Besides, the growth of graphene on Cu is strongly influenced by the partial pressure of hydrogen ($H_2$) [19, 20]; hydrogen acts both as an activator for the decomposition of carbon precursors and as an etching agent that determines the shape and size of the graphene domains. While many studies have focused on the controlled growth of hexagonal graphene, there are few reports on the growth of graphene domains having shapes with lower symmetry, such as pentagonal graphene. Besides, it is still a big challenge to control the orientation of graphene domains during large-scale production, which is important for the development of graphene-based devices.

Here, we report the growth of large-area aligned pentagonal graphene domains on Cu foils by CVD, followed by a systematic study on the shape dependence of graphene domains on both the growth conditions, and the crystallography of the underlying Cu substrate. We found that high-index Cu planes led to the formation of aligned pentagonal graphene domains. In addition, higher partial pressure of $H_2$ accelerated the anisotropic etching of the graphene domain and promoted the formation of pentagonal graphene, but the direction of gas flow did not influence the orientation of the domains.

## 2 Results and discussion

As shown in Fig. 1(a), large-area pentagonal graphene domains with similar orientations were observed on the as-prepared samples. The area covered by aligned pentagonal domains could be as large as 1 $cm^2$ (see Fig. S1 in the Electronic Supplementary Material (ESM)). A pentagonal domain, transferred onto a silicon substrate with a 285-nm oxide layer (285-nm $SiO_2$/Si), shown in Fig. 1(b), has two elongated edges with one inner angle of 60°, while all the other angles are 120°. Figure 1(c) is the transmission electron microscopy

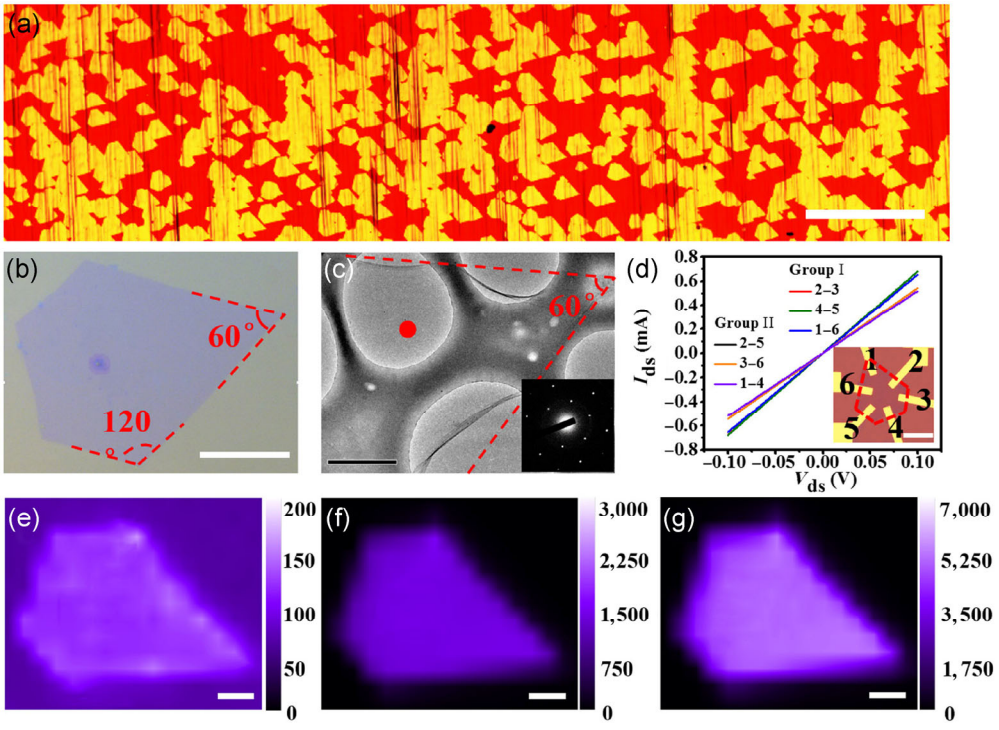


**Figure 1** Pentagonal graphene domains grown on Cu foils. (a) Optical image showing large area pentagonal domains, all with the same orientation, on a Cu foil. Scale bar: 500 μm. (b) Optical image showing an individual domain on a 285 nm $SiO_2$/Si substrate. Scale bar: 50 μm. (c) TEM image showing a part of a domain. Scale bar: 2 μm. Inset is the SAED pattern taken from the area indicated by the dot, showing a single set of hexagonal diffraction spots. (d) Plot of $I_{ds}$ vs. $V_{ds}$ from two groups of electrode pairs. Group I is with neighboring electrodes (1–6, 2–3, 4–5) and Group II is with diagonal electrodes (1–4, 2–5, 3–6). Inset is an optical image of the device. Scale bar: 10 μm. (e)–(g) Raman maps of D-band (1,350 $cm^{-1}$), G-band (1,580 $cm^{-1}$) and 2D-band (2,690 $cm^{-1}$), respectively, of a domain. Scale bar: 1 μm.

(TEM) image of the sharp angle of a pentagonal graphene domain. The crimping of the graphene edges presumably occurred during the transfer process (see the Experimental section). The selected area electron diffraction (SAED) pattern shows a single set of hexagonal diffraction spots (inset of Fig. 1(c)) revealing the single crystalline nature of the pentagonal domain. The electrical properties of the pentagonal graphene domains were studied by fabricating a six-terminal back-gated field effect transistor (see inset of Fig. 1(d) and Fig. S2 in the ESM). As seen in Fig. 1(d), the drain current vs. drain voltage ($I_{ds}$–$V_{ds}$) curves for the two groups (neighboring electrodes and diagonal electrodes) overlap, demonstrating that the electrical properties are uniform over the entire domain [21]. More details on the measurement and the results can be seen in Fig. S2 (in the ESM).

Raman spectroscopy is a direct tool to effectively characterize the quality, thickness, edge attributes and uniformity of graphene domains. A typical Raman spectrum of pentagonal graphene is shown in Fig. S3 (in the ESM). We have carried out Raman mapping on as-grown small pentagonal graphene. Figures 1(e)–1(g) show the Raman maps of the D (1,350 $cm^{-1}$), G (1,580 $cm^{-1}$) and 2D (2,690 $cm^{-1}$) bands. Figure 1(e) shows that the intensity of the D peak ($I_D$) is quite small in the whole region, confirming the high quality of the graphene. Figures 1(f) and 1(g) show the intensities of the G peak ($I_G$) and 2D peaks ($I_{2D}$), respectively. $I_{2D}$ is more than twice the value of $I_G$ over the whole graphene domain, characteristic of uniform monolayer graphene. The ratio of $I_D$ to $I_G$ at the graphene edge is ~0.1, suggesting that the edges consist predominantly of zigzag terminations, which is consistent with results from previous studies [11, 20].

The shapes of the monocrystalline graphene domains grown on Cu foils by CVD, i.e., hexagon or pentagon, depended on the surface crystallography of the underlying Cu grain. Prior to the CVD process, commercial polycrystalline Cu foils were annealed at high temperature that caused the Cu atoms in the polycrystalline Cu foils to rearrange to form large Cu grains, which led to the formation of aligned pentagonal graphene domains on a large scale [22]. Figure 2(a) shows graphene domains on two neighboring Cu grains separated by a grain boundary, where hexagonal domains were formed on the top grain whereas pentagonal domains were observed on the surface of the bottom grain, clearly demonstrating the influence of the underlying Cu grain on the shape of the graphene domains.

In order to establish the relationship between the shapes of the graphene domains and the crystal structure of the Cu grains, electron backscatter diffraction (EBSD) was used to determine the orientation of the underlying Cu crystal. Figure 2(b) is the EBSD image corresponding to Fig. 2(a), showing the distinctly different crystalline surfaces of the two neighboring Cu grains. The top region corresponds to Cu (001) plane, while the bottom region corresponds to Cu (114) plane, which is a high-index plane vicinal to the (001) plane with steps running along the <110> direction. We further confirmed that the underlying Cu crystallographic planes that formed pentagonal

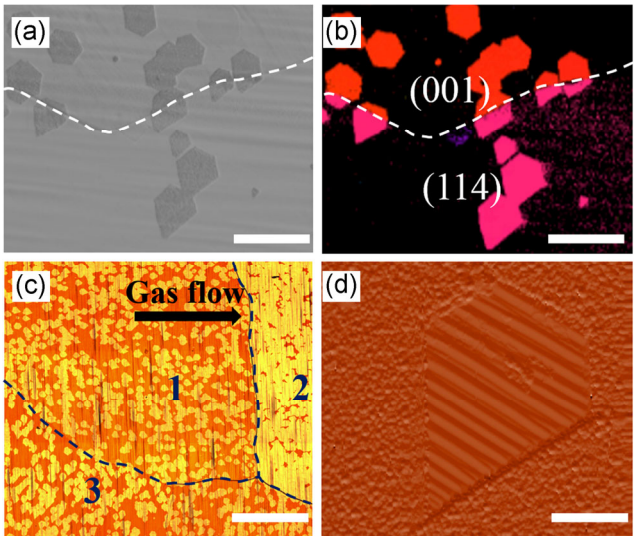


**Figure 2** Dependence of the shape and orientation of graphene domains on the structure of the underlying Cu grains. (a) SEM image showing hexagonal domains on the top Cu grain, and pentagonal domains on the neighboring bottom grain. Scale bar: 200 μm. (b) EBSD mapping showing the crystalline orientation of the two neighboring Cu grains, shown in (a). (c) Optical image showing three neighboring regions with pentagonal domains with three different orientations. The arrow indicates the gas flow direction in CVD. Scale bar: 1 mm. (d) AFM image of a whole pentagonal domain showing the relationship between the graphene orientation and the steps in the underlying Cu crystal surface. Scale bar: 1 μm.

graphene domains are all high-index planes (see details in Fig. S4 in the ESM). These results show that high-index Cu planes lead to the formation of pentagonal domains, and the Cu surfaces underlying each aligned pentagonal graphene share the same planar index.

Additionally, we found that the orientation of the pentagonal graphene domain also depended on the crystallographic orientation of the underlying Cu surfaces. Figure 2(c) shows three neighboring regions with pentagonal graphene domains, where the domain orientations of the Cu grains are different. Figure 2(c) also shows that the orientation of the graphene domain does not depend on the direction of the CVD gas flow, which is in disagreement with previous reports [23]. Atomic force microscopy (AFM) was used to characterize the morphology of an area covered by pentagonal graphene. As seen in Fig. 2(d), the steps in the crystalline lattice of the underlying Cu surface are clearly observed. Interestingly, the symmetry axis of the pentagon is perpendicular to the orientation of these lattice steps, implying that the presence of steps influences the growth rate of graphene in the direction perpendicular the steps. Here, it is interesting to note that due to the oxidation of the bare Cu surface after the CVD process, the steps in the Cu lattice could be observed only in the region covered by graphene.

It is interesting to understand the formation of pentagonal graphene from the point of view of crystal growth theory. If we transform the intrinsic Wulff construction for hexagonal equilibrium to a pentagonal shape, one of the edge energies should be at least twice of the others, which seems unlikely. On the other hand, if the morphology is kinetically controlled, even small differences in kinetic barriers can have a large impact due to the exponential relation between these two parameters [16]. However, measuring growth velocities from experimentally observed shapes (the "inverse Wulff construction") is not straightforward [24], since the origin (sometimes called the "Wulff point"), could in principle be any point inside the crystal. To understand the formation of different shapes, we need to first determine the location of the sites for the nucleation of graphene domains. For highly symmetric shapes, it is reasonable to place it at the geometric center of symmetry, since all other positions would require exceptional fine-tuning of the velocity field to produce a symmetric shape. However, for pentagons, the only assumption that we can confidently make is that the origin lies somewhere on the line of reflection symmetry. However, impurities or lattice defects present on the substrate, which usually act as nucleation sites for the formation of a graphene island, could also function as pathways to transport carbon for the growth of a new layer [25, 26]. To further investigate this possibility, we transferred the graphene layer onto 285 nm $SiO_2$/Si substrates and imaged selectively, those graphene domains with a small second layer, so as to determine the nucleation sites for graphene growth. Here, it is noted that the second layer of graphene may not have the same shape as the first layer since its growth is influenced both by the underlying substrate and the first graphene layer which may alter the concentration of hydrogen around its growing edges. Figure 3(a) is the typical optical image of a hexagonal graphene domain on a 285-nm $SiO_2$/Si substrate, with a second layer located at the center. Figure 3(b) is the corresponding Wulff construction for hexagonal graphene with six-fold symmetry having six edges of the same length, implying an equal growth rate in the six directions. Figures 3(c) and 3(e) show two pentagonal graphene domains with different shapes. It is clearly seen that the six-fold symmetry is lost and the edges of pentagonal domains have different lengths, implying that the growth rates are different in the different directions. We analyzed 108 pentagonal domains and found that these could be classified into two types. Figures 3(c) and 3(d) show domains of Type I and Figs. 3(e) and 3(f) show Type II domains. It was observed that the growth rate of the pentagonal domains was different for the different directions. The fastest growth occurred in the direction along the symmetry axis toward the sharpest angle of the pentagonal graphene domain. Interestingly, Type I, which intuitively seems more symmetric (with only two different edge lengths), is actually produced by a less symmetric growth rate distribution (four distinct values vs. three for Type II). Experimentally, we observed more Type II pentagonal graphene domains than Type I, the ratio of the two domains being 70/38 (see details in Fig. S5 in the ESM).

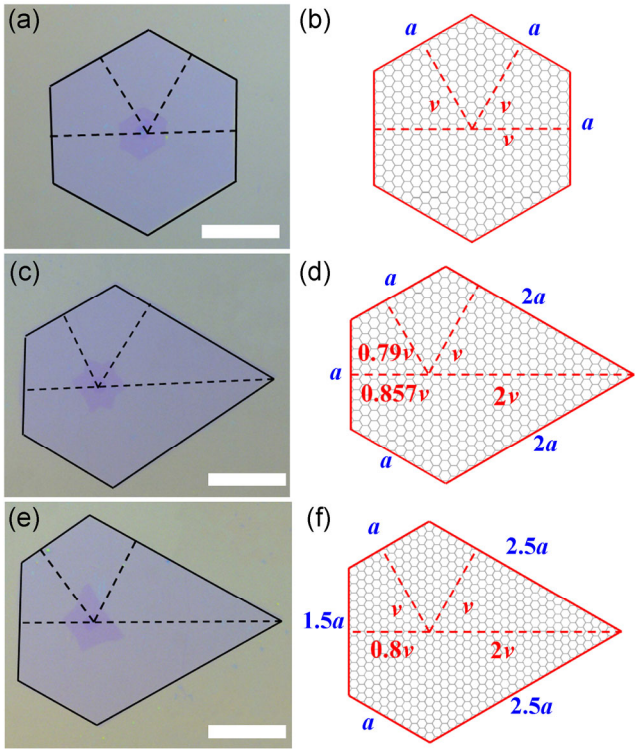


**Figure 3** Analysis of the shapes and growth rates for individual edges for hexagonal and two kinds of pentagonal graphene domains. (a) and (b) Optical image and kinetic Wulff construction for the six-fold symmetry in hexagonal graphene. (c)–(f) Optical image ((c) and (e)) and the corresponding schematic diagram ((d) and (f)) of Type I ((c) and (d)) and Type II ((e) and (f)) pentagonal graphene. Scale bar: 50 μm.

In general, crystals have inherent high symmetries [27–29]. The growth of a hexagonal graphene domain is driven by the intrinsic six-fold symmetry of the graphene lattice. However, for graphene domains on the surface of a crystalline Cu substrate, the interaction between graphene and the substrate may influence the lattice structure of graphene, leading to a reduced symmetry. On a high-index Cu plane, which has a smaller atomic density, a higher surface energy with a greater number of steps and defects, the symmetry can be greatly reduced. Besides, the lattice mismatch between graphene and the Cu lattice is larger for high-index Cu planes. Additionally, the large number of steps will distort the graphene island evolution [17], as a result of which, all the graphene edges cannot be strongly bonded to the metal steps. This gives rise to an optimum growth direction that has the minimum formation energy.

In addition, we found that a high partial pressure of $H_2$ favored the formation of pentagonal graphene. As shown in Figs. 4(a)–4(c), with increased ratio of $H_2$ to $CH_4$ ($H_2/CH_4$), one of the edges of the hexagonal graphene domains stopped growing and eventually disappeared. According to previous studies [12, 20], $H_2$ acts both as a catalyst to promote the surface bound carbon and as an etchant to remove "weak" C–C bonds. In our CVD process, a large amount of $H_2$ improved the growth kinetics of graphene because of the excellent catalytic effect of hydrogen. In parallel, increase in $H_2$ also accelerated the etching, and could be the dominant effect in the growth process. This etching could be highly anisotropic with the Cu substrate playing an important role in the reaction. In sites with high surface energy, the C–C bonds are weaker and more vulnerable to active H atoms, leading to anisotropic etching and the formation of graphene domains with reduced symmetry.

## 3 Conclusions

In summary, we report the growth of oriented large-area pentagonal graphene domains on Cu foils by CVD. High-index Cu planes preferentially formed pentagonal domains. Large areas up to 1 $cm^2$, consisting of similarly oriented pentagonal domains, with their

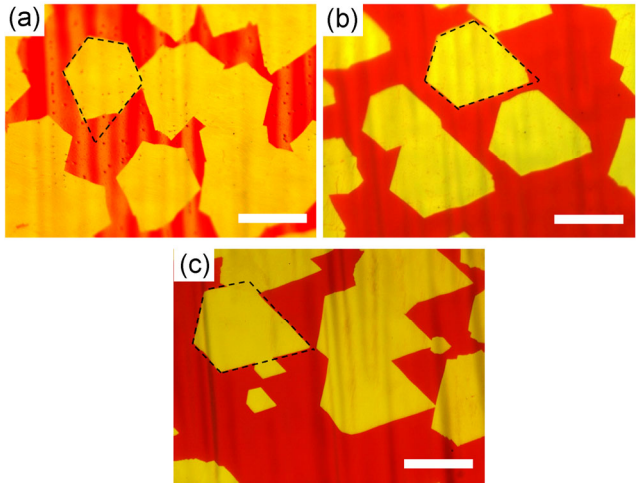


**Figure 4** Optical images of graphene domains on Cu foil showing the evolution of the domain shape with increasing $H_2/CH_4$. (a)–(c) Produced with $H_2$ flow of 45 sccm (a), 60 sccm (b) and 75 sccm (c), Ar flow was fixed at 1,000 sccm and $CH_4$ at 0.2 sccm. Scale bar: 50 μm.

symmetry axis perpendicular to lattice steps on the underlying Cu crystal surface were obtained. This was attributed to favorable growth kinetics in this direction induced by the presence of steps. In addition, $H_2$ was found to promote the formation of pentagonal domains due to anisotropic etching. This work sheds new light on the growth mechanism of graphene by CVD.

## 4 Experimental

### 4.1 Synthesis of pentagonal graphene

Large-area aligned pentagonal graphene was synthesized on a copper foil (25 μm thick, Alfa Aesar Inc) using an atmospheric pressure chemical vapor deposition system with methane (99.999% purity) as the carbon precursor. The copper foil was cleaned in $FeCl_3$/HCl (1 mol/L) solution for 10 s to remove surface oxides and washed with acetone and isopropanol. The blow-dried copper foil was inserted into the CVD chamber. The furnace was heated to 1,050 ˚C in 65 min under a flow of a mixture of argon (250 sccm, 99.999% purity) and hydrogen (18 sccm, 99.999% purity). When the temperature reached 1,050 ˚C, 200 sccm of hydrogen was introduced into the system and maintained for 1.5 h. The growth of large-area aligned pentagonal graphene was carried out with methane (0.26 sccm), hydrogen (75 sccm) and argon (1,000 sccm) for 20 min. Hydrogen flow rates of 45 and 60 sccm have been used to prepare graphene domains with other shapes, as indicated individually. After the reaction, the samples were cooled under a flow of argon and hydrogen.

### 4.2 Transfer of graphene

The following procedure was used for the transfer of graphene: (1) The graphene film grown on the copper foil was coated with poly(methyl methacrylate) (PMMA) (300 nm) by spin coating (3,000 r/min for 30 s); (2) baked in a thermal drying oven at 170 ˚C for 10 min; (3) left overnight in $FeCl_3$/HCl solution (1 mol/L) to etch the copper; (4) the floating film was picked using a clean glass slide and immersed in HCl (0.3 mol/L) for 30 min to remove residual metal ions; (5) cleaned three times with deionized (DI) water ; (6) a target substrate was dipped into the DI water to pick up the film; (7) natural drying for 2 h followed by drying in a blast oven for 30 min to remove water; (8) carefully dipping the grid into acetone to dissolve the PMMA layer; (9) natural drying for 2 h followed by drying in a blast oven for 30 min to remove residual acetone.

### 4.3 Characterization of pentagonal graphene

The morphology of pentagonal graphene was characterized by optical microscopy (LEICA DM2500 M), field emission scanning electron microscopy (FE-SEM) (FEI Quanta 650) and AFM (NanoScope V, Veeco). The orientation of the underlying Cu crystal was determined by EBSD technique. The crystallography of the pentagonal domain was elucidated by field emission transmission electron microscopy (FE-TEM) and SAED test using a JEM2010F(JEOL, Japan). The Raman spectrum and Raman mapping on the as-grown small pentagonal graphene were carried out with a laser excitation wavelength of 532 nm and a step size of 0.5 μm.

### 4.4 Device fabrication and measurement

The six-terminal back-gated graphene field effect transistor (FET) was fabricated using electron-beam lithography (EBL) followed by electron-beam deposition of metal thin films. Six electrodes (5 nm titanium and 50 nm gold) were deposited on the five edges and the sharp corner of the pentagonal graphene. The obtained FETs were characterized using the semiconductor parameter analyzer Agilent B1500 A with probe station, at room temperature and under high vacuum (~$10^{-6}$ mbar) conditions.

## Acknowledgements

This work was supported by the National Natural Science Foundation of China (Nos. 51422204 and 51372132) and the National Basic Research Program of China (No. 2013CB228506).

**Electronic Supplementary Material**: Supplementary material (supplementary figures (Figs. S1–S5) and supplementary text about electrical transport properties,

Raman spectrum and EBSD characterization results of the underlying Cu grains of pentagonal domains) is available in the online version of this article at http://dx.doi.org/10.1007/s12274-016-1107-9.

## References


[1] Neto, A. H. C.; Guinea, F.; Peres, N. M. R.; Novoselov, K. S.; Geim, A. K. The electronic properties of graphene. *Rev. Mod. Phys.* **2009**, *81*, 109–162.

[2] Allen, M. J.; Tung, V. C.; Kaner, R. B. Honeycomb carbon: A review of graphene. *Chem. Rev.* **2010**, *110*, 132–145.

[3] Yin, Z. Y.; Zhu, J. X.; He, Q. Y.; Cao, X. H.; Tan, C. L.; Chen, H. Y.; Yan, Q. Y.; Zhang, H. Graphene-based materials for solar cell applications. *Adv. Energy Mater.* **2014**, *4*, 1300574.

[4] Zhu, J. X.; Yang, D.; Yin, Z. Y.; Yan, Q. Y.; Zhang, H. Graphene and graphene-based materials for energy storage applications. *Small* **2014**, *10*, 3480–3498.

[5] Huang, X.; Qi, X. Y.; Boey, F.; Zhang, H. Graphene-based composites. *Chem. Soc. Rev.* **2012**, *41*, 666–686.

[6] Cao, X. H.; Yin, Z. Y.; Zhang, H. Three-dimensional graphene materials: Preparation, structures and application in supercapacitors. *Energy Environ. Sci.* **2014**, *7*, 1850–1865.

[7] Zhang, W. L.; Xie, H. H.; Zhang, R. F.; Jian, M. Q.; Wang, C. Y.; Zheng, Q. S.; Wei, F.; Zhang, Y. Y. Synthesis of three-dimensional carbon nanotube/graphene hybrid materials by a two-step chemical vapor deposition process. *Carbon* **2015**, *86*, 358–362.

[8] Dai, B. Y.; Fu, L.; Zou, Z. Y.; Wang, M.; Xu, H. T.; Wang, S.; Liu, Z. F. Rational design of a binary metal alloy for chemical vapour deposition growth of uniform single-layer graphene. *Nat. Commun.* **2011**, *2*, 522.

[9] Gao, L. B.; Ren, W. C.; Xu, H. L.; Jin, L.; Wang, Z. X.; Ma, T.; Ma, L. P.; Zhang, Z. Y.; Fu, Q.; Peng, L. M. et al. Repeated growth and bubbling transfer of graphene with millimetre-size single-crystal grains using platinum. *Nat. Commun.* **2012**, *3*, 699.

[10] Li, X. S.; Cai, W. W.; Colombo, L.; Ruoff, R. S. Evolution of graphene growth on Ni and Cu by carbon isotope labeling. *Nano Lett.* **2009**, *9*, 4268–4272.

[11] Luo, Z. T.; Kim, S.; Kawamoto, N.; Rappe, A. M.; Johnson, A. T. C. Growth mechanism of hexagonal-shape graphene flakes with zigzag edges. *Acs Nano* **2011**, *5*, 9154–9160.

[12] Yan, Z.; Lin, J.; Peng, Z. W.; Sun, Z. Z.; Zhu, Y.; Li, L.; Xiang, C. S.; Samuel, E. L.; Kittrell, C.; Tour, J. M. Toward the synthesis of wafer-scale single-crystal graphene on copper foils. *Acs Nano* **2012**, *6*, 9110–9117.

[13] Zhang, Y.; Zhang, L. Y.; Kim, P.; Ge, M. Y.; Li, Z.; Zhou, C. W. Vapor trapping growth of single-crystalline graphene flowers: Synthesis, morphology, and electronic properties. *Nano Lett.* **2012**, *12*, 2810–2816.

[14] Wu, Y. A.; Robertson, A. W.; Schäffel, F.; Speller, S. C.; Warner, J. H. Aligned rectangular few-layer graphene domains on copper surfaces. *Chem. Mater.* **2011**, *23*, 4543–4547.

[15] Liu, J. W.; Wu, J.; Edwards, C. M.; Berrie, C. L.; Moore, D.; Chen, Z. J.; Maroni, V. A.; Paranthaman, M. P.; Goyal, A. Triangular graphene grain growth on cube-textured Cu substrates. *Adv. Funct. Mater.* **2011**, *21*, 3868–3874.

[16] Artyukhov, V. I.; Hao, Y. F.; Ruoff, R. S.; Yakobson, B. I. Breaking of symmetry in graphene growth on metal substrates. *Phys. Rev. Lett.* **2015**, *114*, 115502.

[17] Wofford, J. M.; Nie, S.; McCarty, K. F.; Bartelt, N. C.; Dubon, O. D. Graphene islands on Cu foils: The interplay between shape, orientation, and defects. *Nano Lett.* **2010**, *10*, 4890–4896.

[18] Nguyen, V. L.; Shin, B. G.; Duong, D. L.; Kim, S. T.; Perello, D.; Lim, Y. J.; Yuan, Q. H.; Ding, F.; Jeong, H. Y.; Shin, H. S. et al. Seamless stitching of graphene domains on polished copper (111) foil. *Adv. Mater.* **2015**, *27*, 1376–1382.

[19] Zhang, Y.; Li, Z.; Kim, P.; Zhang, L. Y.; Zhou, C. W. Anisotropic hydrogen etching of chemical vapor deposited graphene. *ACS Nano* **2012**, *6*, 126–132.

[20] Vlassiouk, I.; Regmi, M.; Fulvio, P.; Dai, S.; Datskos, P.; Eres, G.; Smirnov, S. Role of hydrogen in chemical vapor deposition growth of large single-crystal graphene. *ACS Nano* **2011**, *5*, 6069–6076.

[21] Yan, Z.; Liu, Y. Y.; Lin, J.; Peng, Z. W.; Wang, G.; Pembroke, E.; Zhou, H. Q.; Xiang, C. S.; Raji, A. R. O.; Samuel, E. L. G. et al. Hexagonal graphene onion rings. *J. Am. Chem. Soc.* **2013**, *135*, 10755–10762.

[22] Sekerka, R. F. Equilibrium and growth shapes of crystals: How do they differ and why should we care? *Cryst. Res. Technol.* **2005**, *40*, 291–306.

[23] Jung, D. H.; Kang, C.; Yoon, D.; Cheong, H.; Lee, J. S. Anisotropic behavior of hydrogen in the formation of pentagonal graphene domains. *Carbon* **2015**, *89*, 242–248.

[24] Artyukhov, V. I.; Liu, Y. Y.; Yakobson, B. I. Equilibrium at the edge and atomistic mechanisms of graphene growth. *Proc. Natl. Acad. Sci. USA* **2012**, *109*, 15136–15140.

[25] Han, G. H.; Güneş, F.; Bae, J. J.; Kim, E. S.; Chae, S. J.; Shin, H.-J.; Choi, J.-Y.; Pribat, D.; Lee, Y. H. Influence of copper morphology in forming nucleation seeds for graphene growth. *Nano Lett.* **2011**, *11*, 4144–4148.

[26] Ma, T.; Ren, W. C.; Zhang, X. Y.; Liu, Z. B.; Gao, Y.; Yin,

L. C.; Ma, X. L.; Ding, F.; Cheng, H. M. Edge-controlled growth and kinetics of single-crystal graphene domains by chemical vapor deposition. *Proc. Natl. Acad. Sci. USA* **2013**, *110*, 20386–20391.

[27] Yuan, Q. H.; Yakobson, B. I.; Ding, F. Edge-catalyst wetting and orientation control of graphene growth by chemical vapor deposition growth. *J. Phys. Chem. Lett.* **2014**, *5*, 3093–3099.

[28] Hayashi, K.; Sato, S.; Yokoyama, N. Anisotropic graphene growth accompanied by step bunching on a dynamic copper surface. *Nanotechnology* **2013**, *24*, 025603.

[29] Yan, Z.; Liu, Y. Y.; Ju, L.; Peng, Z. W.; Lin, J.; Wang, G.; Zhou, H. Q.; Xiang, C. S.; Samuel, E. L. G.; Kittrell, C. et al. Large hexagonal Bi- and trilayer graphene single crystals with varied interlayer rotations. *Angew. Chem., Int. Ed.* **2014**, *53*, 1565–1569.